# Climatic forcing and flood frequency

**C. GALIMBERTI-AGHION & P. BURLANDO**

*Inst. of Hydromechanics and Water Resour. Manag., ETH Zurich, CH 8093,Switzerland, e-mail:* cecilia@ihw.baug.ethz.ch

## ABSTRACT

The apparently increasing frequency of hydrological extremes in recent years boosted once again the speculation on the effects of climate change on natural hazards. Despite the scientific community has been addressing this topic for some years, the debate often generated contradictory opinions. Far from proposing a decisive answer, we present here an investigation that focuses on the effects of changing rainfall regime on flood frequency regime. Specifically, climate scenarios derived by stochastic downscaling of General Circulation Models (GCMs) predictions have been used to simulate the hydrologic response at the catchment scale, highlighting the potential effects of a non-stationary scenario accounting for a transient evolution of the climatic forcing. Long-term simulations of storm rainfall have been thus generated to investigate modifications of internal structure of rainfall events, and how these affect the generation and the occurrence of floods. Fine resolution simulated rainfall has been used first to investigate how the storm risk is expected to change, and second as input to an event-based lumped rainfall-runoff model, that has been calibrated on observed events. Results are discussed for the Mediterranean Sieve river basin (Italy), exposed to potential enhancement of climate change effects on precipitation due to orography. Hydrograph characteristics and annual flood series for a transient scenario of about hundred years are analyzed to argue about changes induced by large scale forcing as predicted by GCMs for the region under study. The growth curve of peak flows is also compared to actual flood regime to suggest potential implications on engineering design and on protection policies. In this respect, some discussion about inherent uncertainties as compared to detected changes is also challenged.

# 1 INTRODUCTION

In recent times the scientific community, policy makers and public opinion have shown a considerable concern to the issue of global climate change caused by the increase of the atmospheric concentration of the so-called greenhouse gases. Such concern originates from the growing awareness that the natural evolution of Earth's climate can be significantly impacted by anthropogenic forcings (*Mitchell*, 1989; *IPCC*, 1995a, b and c).

In particular, hydrological processes are most likely to be affected by long-term climate variations, because of the relationship that closely links them to atmospheric circulation patterns and climatic variables. In the past two decades a substantial research effort has been devoted to assess the effects of potential climate change on hydrologic cycle and water resources availability (see e.g. *Nemec and Schaake*, 1982; *Klemes*, 1985; *Cohen*, 1986; *Askew*, 1987; *Gleick*, 1987, 1989; *Ripley*, 1987; *Mimikou and Kouvopoulos*, 1991; *Loukas and Quick*, 1996; *Strzepek and Yates*, 1997), mostly by evaluating significant shifts of the mean climate. Conversely, limited attention has been paid in exploring also changes in variability of climatic variables (see e.g. *Burlando and Rosso*, 1991; *Mearns et al.*, 1997; *Semenov and Barrow*, 1997), despite "*it is extremely unlikely that shifts in the means of weather distributions will take place without shifts in the tails*" (*Burton*, 1997). Similarly the scientific literature about climate change impact assessment has not considered to a detailed extent the effects on hydrologic extremes. For instance, despite flooding phenomena represent a major hazard because of damages and high recovering costs, only a limited number of examples of flood analysis under climate change scenarios have been reported in the literature.

Among these, *Lettenmaier and Gan* (1990) carried out a pioneer study aimed at investigating the sensitivity to global warming of annual maximum daily flow distribution of the Sacramento-San Joaquin river basin. In this study they used climate projections from General Circulation Models (GCMs) as direct input to hydrologic models. GCMs provide nowadays the most sophisticated, and yet flexible, tool to predict future atmospheric circulation patterns under modified atmospheric conditions; however, they still denote serious limitations in modelling accurately hydrological processes such as streamflow. This approach shows therefore some main inconsistencies, due to the existing incompatibility between the too coarse spatial, and sometime temporal, resolution of GCMs' simulations and the local scales required by hydrologic models to yield consistent and reliable results (*Gleick*, 1989; IPCC, 1994; *Semenov and Barrow*, 1997). Moreover, currently available GCMs suffer from an extremely simple parametrization of hydrologic processes, which does not allow a detailed simulation of mesoscale forcings induced by topographic and land surface complexity. Accordingly several disaggregation techniques have been devised (see *Giorgi and Mearns*, 1991 for a detailed review) in order to simulate regional climates driven by large scale predictions of GCMs, but at the same time able to account for climate variability and catchment characteristics.

A downscaling technique has been followed for instance by *Hughes et al.* (1993), who disaggregated the precipitation amounts to the regional scale via a stochastic approach based on a weather state classification scheme. The so-downscaled precipitation was then used to input a rainfall-runoff model to assess the variations of flood frequency distributions under altered climate in two basins of US northwestern region. A different disaggregation method, first proposed by *Epstein and Ramirez* (1994), has been recently used *by Loukas and Quick* (1999) to adjust the mean monthly values of precipitation and temperature according to GCMs experiments, yet without incorporating the variability of the two simulated variables. Subsequently, the authors evaluated the effects induced by climate change into nine flood parameters of the Upper Campbell and Illecillewaet Canadian catchments by applying the watershed model developed at the University of British Columbia (*Quick*, 1995).

Common features, and limitations, to all the cited works, as well as to other studies dealing with streamflow (*Nash and Gleick*, 1991; *Epstein and Ramirez*, 1994), are the evaluation of discharge values at a resolution not finer than daily and the consideration of steady-state climatic scenarios derived from equilibrium experiments of GCMs. The former aspect constrains the potential practical applicability of these studies to large catchments, which are characterized by long response time, so limiting conclusions with respect to mesoscale and flash-flood prone basins, where hourly or, if possible, sub-hourly estimation of the hydrograph is required. The second assumption involves that output data from GCMs are produced by accounting for a constant atmospheric concentration of carbon-dioxide, commonly indicated as $1xCO_2$ for present climate and $2xCO_2$ for the most typical future climate experiments. Therefore hydrologic simulations can account only for differences between two stationary climates, without considering that transient scenarios of climate evolution, due to continuously increasing $CO_2$ concentration, could lead to different reactions of hydrologic systems, eventually showing both enhanced and smoothed patterns as compared with steady climate simulations.

The present work tries to overcome the above outlined restrictions. The simple methodology that is here introduced aims at investigating how global predictions of climate change affect flood frequency, as evaluated on a space-time scale of interest for engineering design problems in mesoscale catchments. Unlike previous studies, the approach hereafter presented makes use of a transient climate change scenario as starting point for further simulations. Such scenario, provided by the last generation of GCMs, accounts for the doubling of $CO_2$ atmospheric concentration by continuously, time-dependently increasing the percentage of greenhouse gases, without having an abrupt and quite unrealistic change between future projections and present climate conditions. Moreover, in order to avoid as much as possible hypothetical climatic predictions, the adopted GCM scenario accounts also for the action of sulphate aerosols, the cooling mechanism of which is recognized to be the second most influent anthropogenic forcing component in the atmosphere after greenhouse gases (*Mitchell et al.*, 1995). Furthermore, a second innovative aspect is introduced, in that GCMs output are used to drive local changes by means of a stochastic downscaling technique, first introduced by *Burlando and Rosso* (1991), which allows to account for process variability when simulating climate change impacts at the basin scale. As described in the following, long precipitation and temperature series at a hourly time step have been accordingly generated to drive a basin scale rainfall-runoff model, used to investigate climate change impacts on flood regimes.

## 2 METHODOLOGICAL FRAMEWORK

The assessment of impacts of climate change on streamflow and, generally speaking, on hydrologic processes at local scale, can be essentially categorized in two different approaches. The first relies on statistical methods to derive empirical relationships either between climatic variables (usually precipitation and temperature) and streamflow, or between large scale climatic patterns and hydrologic variables. The second one makes use of either physically-based or conceptual mathematical models of hydrologic processes, which are driven by properly downscaled input variables provided by GCMs scenarios.

The methodological approach followed in the present note belongs to the second category, as it is clarified in Figure 1. Although several hydrologic models are included, the methodology is structured in form of a cascade of simple procedures that outline a straightforward and easy-to-apply tool. Specifically, four main parts characterize the methodology, hereafter briefly described.

First, GCMs simulations have been selected (Figure 1A) to describe rainfall and temperature patterns under a control and a transient climate scenario. Both scenarios are time-dependent, but, while the former is assumed to be in a steady state representing the current climate, the latter is dominated by non-stationary conditions, which account for a gradually increased concentration of equivalent $CO_2$ in the atmosphere.

Secondly, GCMs direct outputs have been disaggregated to the regional scale (Figure 1B) by means of downscaling techniques that make use of a stochastic rainfall model (the Neyman-Scott Rectangular Pulses model, NSRP) and of a simple linear AutoRegressive model for the simulation of rainfall and temperature time series respectively.

The so-generated series have been then given as input to a conceptual hydrologic model - the Precipitation-Runoff Modelling System, PRMS, (*Leavesley et al.*, 1983 and 1995), - in order to perform a continuous simulation of catchment state evolution, so obtaining daily discharge and soil moisture conditions (Figure 1C). Such simulations allowed, on one hand, the screening of the most meaningful flood generating rainfall events, and provided, on the other hand, the initial state of the catchment.

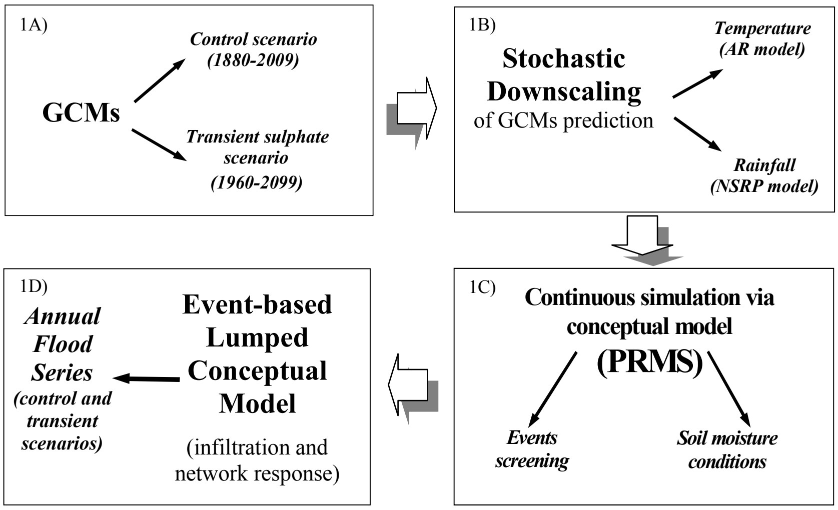


Figure 1: Work methodology

This was necessary to drive, as fourth step, a lumped event-based rainfall-runoff model, in order to describe the evolution of individual flood hydrographs for each selected rainfall event under both the control and the transient scenario (Figure 1D). Annual maxima of flood peaks have been finally collected to obtain a generated Annual Flood Series.

In the next paragraphs the study area is first shortly outlined, followed by a detailed description of the adopted hydrologic models.

## 2.1 Basin case study and weather input data

The Sieve river basin has been selected as a case study. The basin covers an area of 831 km$^2$ and is located in the upper part of the Arno river basin (Figure 2), Central Italy, at approximately 43° N of latitude and 11°E of longitude, representing this an area which is believed to be particularly exposed to potential enhancement of climate change effects on precipitation regime and, as a consequence, on flood regime. Moreover, the Sieve river basin is located in a region particularly flood prone, since it is subject to the high variability of Mediterranean climate, with intense rainfall in fall season and dry summers, but yet in some cases characterized by heavy storms. This high variability is also reflected in the discharge regime, which shows extremely different flow patterns depending on the period within the year.

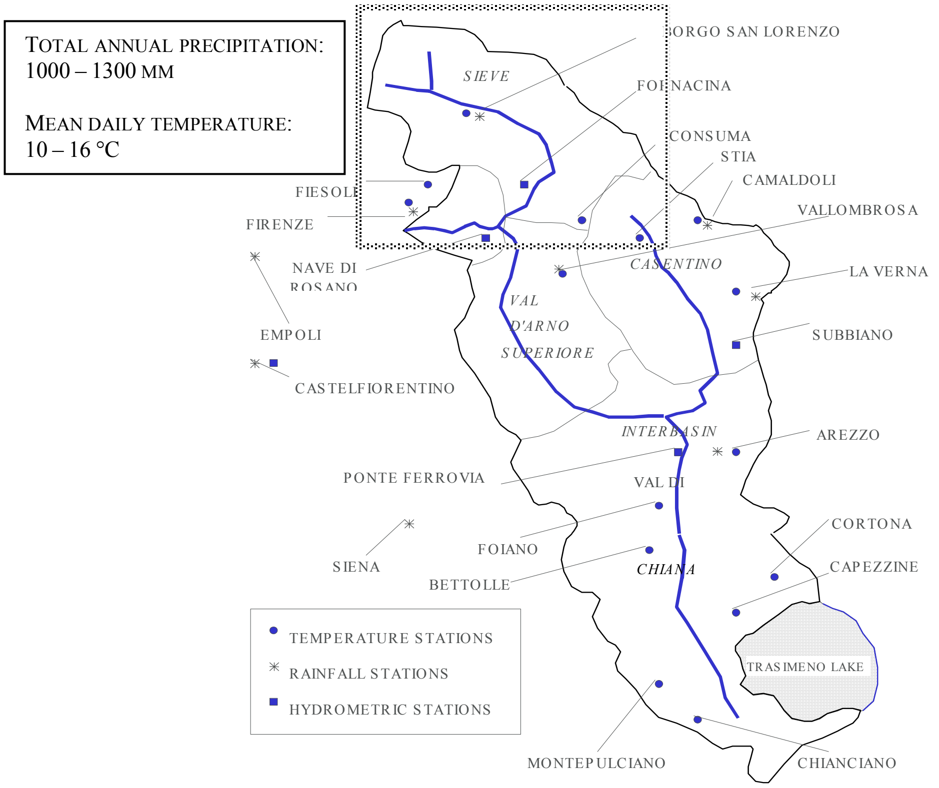


Figure 2: Map of rainfall, temperature and hydrometric stations in the Arno river basin; the Sieve river basin is located in the upper part.

In the present study observed rainfall and temperature data are provided by the climatological Borgo S.Lorenzo station, located in the central part of the basin at 193 m a.s.l.. Discharge measurements are supplied by the station located at the outlet of the basin in Fornacina. Table 1 lists the type and record length of available data of the considered stations.

Climate change simulations to define precipitation and temperature scenarios under climate change have been provided by the GCMs outputs of the latest version of the HADCM2 model (*Mitchell et al.*, 1995), implemented by the Hadley Center for Climate Prediction and Research of the United Kingdom Meteorological Office (UKMO). In particular, two experiments of this model have been used (see Table 2 for a more detailed description): the CON integration, which is expected to reproduce the present climate by keeping $CO_2$ concentration constant, and the SUL integration, in which both greenhouses gases and the direct radiative effect of sulphate aerosols are represented. All experiments are performed at a grid resolution of 2.5° x 3.75° in latitude and longitude.

| *Borgo S.Lorenzo rainfall station* | | |
|---|---|---|
| *Type of data* | *Time resolution* | *Record length* |
| rainfall depths | 20’ | 1962-1986 |
| max. temperature | daily | 1958-1989 |
| min. temperature | daily | 1958-1989 |
| *Fornacina hydrometric station* | | |
| *Type of data* | | *Record length* |
| peak flows | | 1958-1988 |
| flood hydrographs | | selected events betw. |

Table 1: Type and temporal length of available data at Borgo S.Lorenzo station and Fornacina cross-section.

| *GCM experiment* | *Type* | *Description* |
|---|---|---|
| HADCM2CON | transient | CONtrol integration over a time span of 240 years (1860-2099) for monthly data. It is characterized by a constant atmospheric forcing which simulates the concentration of greenhouse gases of the present climate. Variables simulated in this run and used in the study are monthly mean maximum and minimum temperature [°C] and monthly mean daily precipitation [mm/day]. |
| HADCM2SUL | transient | greenhouse gases and SULphate aerosols integration over a time span of 240 years (1860-2099) for monthly data. The forcing component is estimated on historical observation until 1990 and afterwards increased of about 1% $yr^{-1}$, based on IPCC scenario IS92a. Variables simulated in this run and used in the study are monthly mean maximum and minimum temperature [°C] and monthly mean daily precipitation [mm/day]. |

Table 2: Description of the CON and SUL experiments of the HADCM2 model

## 2.2 Stochastic downscaling

As already mentioned, the direct use of GCMs results into hydrologic model is not advisable because of different resolutions at which the two types of models are conceived and run. In the present work, the problem of scale consistency between the local rainfall scenario and global climate change simulations has been faced by means of the stochastic downscaling technique proposed by *Burlando and Rosso* (1990, 1991). This technique provides an analytical framework to modify, on the basis of GCMs derived climate trend predictions, the parameters of a point rainfall stochastic model that was originally estimated on local historical observations. A similar approach has been also adopted to reproduce future local scenarios of maximum and minimum temperature (*Burlando et. al.*, 1997).

### 2.2.1 Precipitation scenarios

Following the mentioned approach (*Burlando and Rosso*, 1990; 1991), local modifications of rainfall patterns are investigated combining GCMs output and non-stationary rainfall analysis by means of scaling concepts and of a rainfall stochastic model. This is the Neyman-Scott Rectangular Pulses (NSRP) model (Figure 3), which extensive results reported in literature showed to be able to capture the properties of both the continuous and the extremal process (*Burlando*, 1989; *Burlando and Rosso*, 1993; *Cowpertwait*, 1994; 1995; *Cowpertwait et al.*, 1996). The model is based on Poisson arrivals of storms, being associated to each arrival a cluster of rectangular pulses of random height and duration, randomly displaced from the cluster origin.

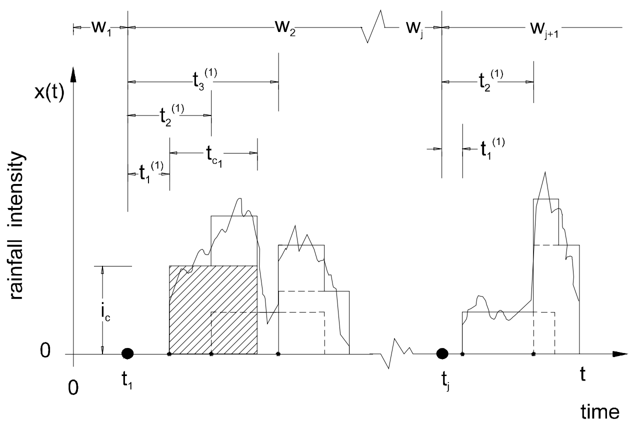


$w_j$ = interarrival time of events (pulses)
$t_1^{(j)}$ = displacement of the j-th cell from the cluster center
$t_{c_i}$ = duration of the i-th pulse
$i_{c_i}$ = intensity of the i-th pulse

Figure 3: The Neyman-Scott Rectangular Pulses Model

The superposition of these pulses provides the description of the storm profile. In the earliest model formulation it is assumed that both the intensity and the duration of a pulse are iid exponentially distributed, being displaced from the cluster origin according to an exponential distribution, and being the number of cells geometrically distributed. Such a structure yields a five parameter model, which must be calibrated by fitting observed statistics to analytical expressions of the second-order properties, as reported, e.g., by *Burlando* (1989). Table 3 displays the parameters so estimated for the station of Borgo S.Lorenzo on a monthly basis.

| | Borgo S.Lorenzo station (1962-1986) | | | | |
|---|---|---|---|---|---|
| | $\lambda$ | $\delta$ | $\mu_\chi$ | $\nu$ | $\beta$ |
| MONTH | [-] | [h] | [mm/h] | [-] | [$h^{-1}$] |
| January | 0.0111 | 1.202 | 8.793 | 1.036 | 0.073 |
| February | 0.0117 | 1.083 | 8.383 | 1.160 | 0.086 |
| March | 0.0112 | 1.198 | 8.847 | 1.031 | 0.073 |
| April | 0.0101 | 0.604 | 13.315 | 1.300 | 0.106 |
| May | 0.0129 | 0.580 | 4.806 | 2.347 | 0.086 |
| June | 0.0075 | 0.796 | 4.374 | 2.578 | 0.064 |
| July | 0.0054 | 0.320 | 3.735 | 5.411 | 0.181 |
| August | 0.0067 | 0.312 | 4.308 | 11.525 | 0.183 |
| September | 0.0051 | 0.403 | 6.888 | 7.198 | 0.033 |
| October | 0.0083 | 0.423 | 13.460 | 2.411 | 0.125 |
| November | 0.0108 | 0.578 | 12.373 | 2.265 | 0.126 |
| December | 0.0091 | 0.929 | 11.934 | 1.218 | 0.067 |

Table 3: Parameters values of NSRP model for Borgo S.Lorenzo station

By using these parameters 50 years of point hourly precipitation have been generated and then compared to observations in terms of statistical and extreme properties in order to validate the NSRP model. In both cases the stochastic model showed a satisfactory performance in reproducing the main characteristics of the historical process, so providing a quite reliable tool for continuous simulation of rainfall time series.

As an example, Figure 4 illustrates the agreement between the observed and the simulated DDF (Depth-Duration-Frequency) curves for intervals of aggregation of 1 and 24 hours respectively.

| *T = 1h* | | | |
|---|---|---|---|
| *Month* | *Δmean (%)* | *Δvariance (%)* | *Δcorr(1) (%)* |
| August | 2.8 | 2.6 | 4.9 |
| November | -13.4 | -15.9 | -9.2 |
| *T = 24h* | | | |
| *Month* | *Δmean (%)* | *Δvariance (%)* | *Δcorr(1) (%)* |
| August | -3.0 | 5.1 | -31.8 |
| November | -11.4 | -10.8 | -13.2 |

Table 4: Differences in percentage of sample mean, variance and correlation coefficient at lag 1 between observed and NSRP simulated rainfall series.

Furthermore Table 4 reports the quantitative difference between some observed and simulated important statistical properties for the months of August and November. The adequate fitting of generated rainfall with respect to the observed dataset allows to consider the generated series as representative at a local scale of the precipitation process under the historical and, consequently, also under the control scenario.

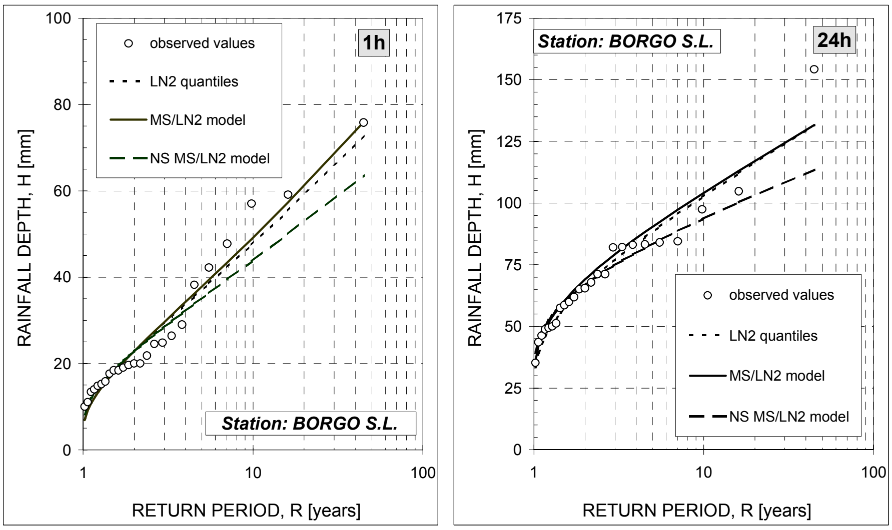


Figure 4: Comparison between observed and NSRP simulated DDF curves for 1 and 24 hours temporal intervals at Borgo S.Lorenzo station.

The combination of second order properties – mean, variance and covariance – as well as of the scale of fluctuation first derived by *Rodriguez-Iturbe* (1986) with a power law describing the relationship between the first and the second order central moments, allowed *Burlando and Rosso* (1991) to derive a few analytical relationships useful to estimate the value of NSRP parameters as modified by climate change scenarios. Referring the reader to the original paper by these authors for a detailed description of the procedure, such relationships can be shortly written as

$$\frac{\lambda_{nxCO_2}}{\lambda_{control}} = k_\lambda \, ; \quad \frac{\mu_{nxCO_2}}{\mu_{control}} = k_\mu \, ; \quad \frac{\delta_{nxCO_2}}{\delta_{control}} = k_\delta \, ; \quad \frac{\beta_{nxCO_2}}{\beta_{control}} = k_\beta \, ; \quad \frac{\nu_{nxCO_2}}{\nu_{control}} = 1 \qquad (1.)$$

being λ, μ, δ, β and ν the NSRP parameters and describing respectively the Poisson rate of storm arrival (λ), the mean intensity and duration of a pulse (μ and δ), the mean displacement of a cell from the cluster origin ($\beta^{-1}$) and the mean number of cells in a cluster (ν), supposed to be constant under the control and the transient scenario.

Without entering unnecessary further details, it is important to notice that the complete expressions of eqn 1 are function of the model parameters themselves, of the parameters of the above mentioned power law linking central moments, and of the ratio:

$$\frac{\overline{P}_{(n\times \mathrm{CO}_2)}}{\overline{P}_{(\mathrm{control})}} = K_m \qquad (2.)$$

Such ratio quantifies the change between the mean daily precipitation under the enhanced $CO_2$ scenario, $\overline{P}_{(n\times CO_2)}$, and the actual mean daily precipitation, $\overline{P}_{(control)}$, corresponding to the control scenario, both obtained from GCMs simulations. In this way the climate change trend as simulated by GCMs are included into the reparameterization expressions of eqn 1. Therefore the reparameterization procedure requires a minimum of information coming from GCMs, with the purpose of limiting error and bias propagation that arise from a direct use of GCMs output in basin hydrological models. Moreover, the so reparameterized NSRP model allows the generation of rainfall scenarios for which not only changes in the mean process can be detected, but also changes in its variability can be accounted for.

The above summarized procedure has been applied to Borgo S.Lorenzo station. The NSRP parameters estimated from historical statistics (see Table 3), and representing the control scenario, have been then rescaled for each month on a decadic basis in order to account for climate change trends outlined by GCMs transient predictions. In Figure 5, 6 and 7 some examples are reported of how NSRP parameters are expected to vary within the year given a specific decade (Figure 5) or over the next century given two sample months (Figures 6 and 7). At a first look one notices that parameters values can also be subject to strong fluctuations, depending on the month or decade. This behaviour underlines how crucial is to consider a transient climatic forcing in order to achieve the most realistic depiction of climate change at a local scale.

After the NSRP model reparameterization, 50 years of hourly rainfall have been generated for each of the 11 decades going from 1990 to 2099, being the latest the one until GCMs simulations are available. Then, 10 years of data out of the 50 years have been randomly collected per decade, so obtaining a series of 110 years of simulated precipitation which represents the transient rainfall scenario downscaled at the basin scale.

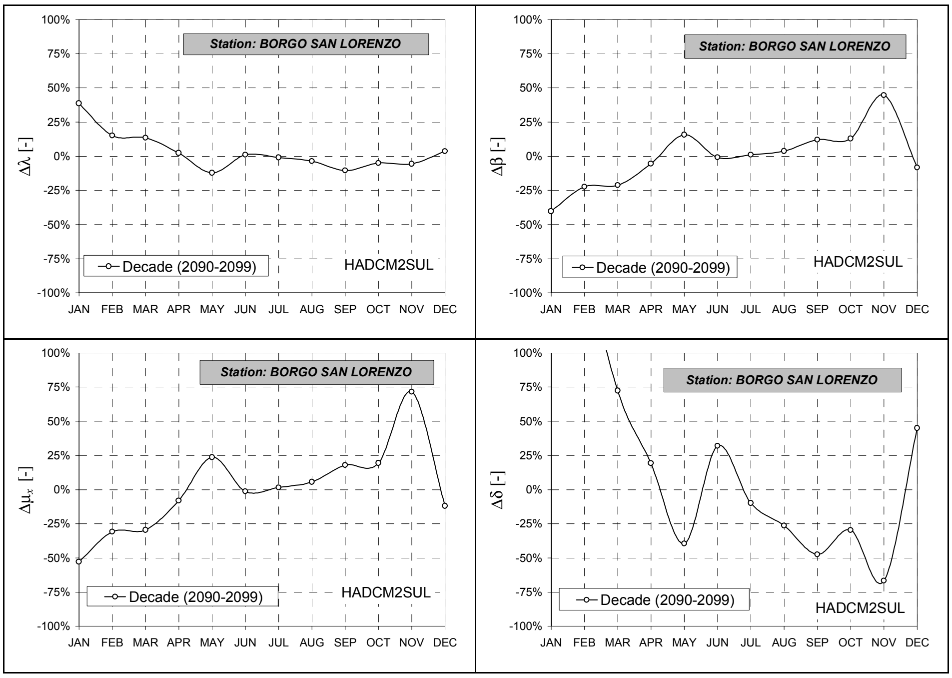


Figure 5: Monthly variation of NSRP model parameters during the 2090-2099 decade in Borgo S.Lorenzo station under the HADCM2SUL scenario.

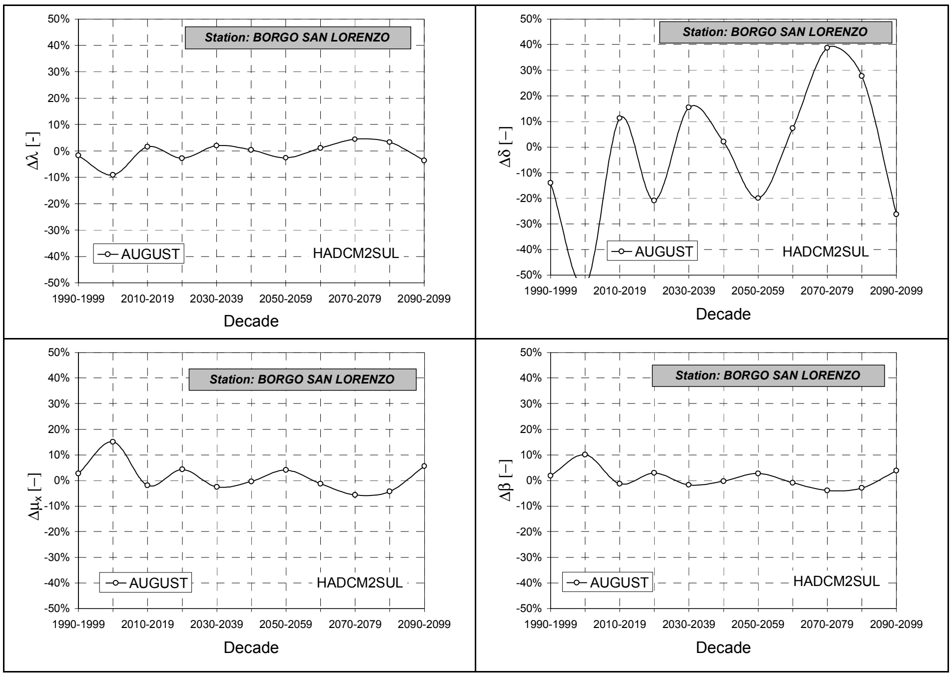


Figure 6: Decadic variation of NSRP model parameters in Borgo S.Lorenzo station for the month of August under the HADCM2SUL scenario.

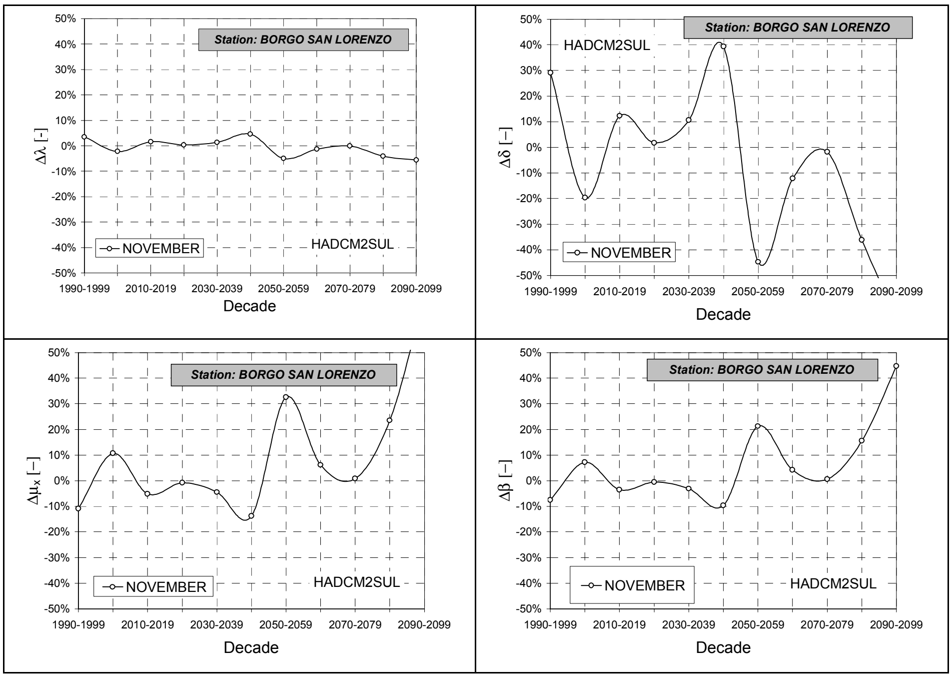


Figure 7: Decadic variations of NSRP model parameters in Borgo S.Lorenzo station for the month of November under the HADCM2SUL scenario.

### 2.2.2 Temperature scenarios

The overall procedure to analyze climate change impacts on flood regime requires to define also temperature scenarios, which drive together with the precipitation ones the hydrologic model describing the catchment state evolution. A scenario generator that accounts for mutual influence of temperature and precipitation would be in this respect the proper tool. It has been indeed shown that relationships linking daily temperature and precipitation can be found (see, e.g., *Brandsma and Buishand*, 1999). Unfortunately, in the specific case of Central Italy such relationship were proved not to hold (*Brandsma and Buishand*, 1997). As a consequence it has been decided to assume the two processes as independent.

Accordingly, a stochastic downscaling methodology independent from previously generated precipitation time series has been used to reproduce a basin-scaled temperature scenarios for enhanced and constant $CO_2$ atmospheric concentration. For the control scenario, observed records of daily maximum and minimum temperature at Borgo S.Lorenzo station have provided the necessary data set to calibrate a linear stochastic model for each series. The choice of this kind of representation is motivated by the efficiency and robustness that has generally shown in modelling hydrological time series in a wide range of applications. Specifically, a simple AutoRegressive model of *p-th* order, AR(*p*), has been used, as it proved to be the most efficient among others to reproduce accurately the variable of interest. After some calibration exercise an AR(5) and AR(4) have been determined to provide a correct reproduction of the maximum and the minimum temperature respectively. This is well illustrated by Figure 8 and 9 reporting the fitting of generated autocorrelation functions and sample densities to the equivalent functions derived from observed data.

The same model has been also used for the transient scenario, by preliminarily reparametrizing the location parameter of the probability distribution of the historical series. This was done, coherently with precipitation, on a 10-years step adding to the observed sample mean the difference $\Delta T$ of temperature that GCM predicts between the mean temperature of the control scenario, $\overline{T}_{(control)}$, and the mean temperature of the transient scenario in a specific decade $n$, $\overline{T}_{(n \times CO_2)}$, that is:

$$\Delta T = \overline{T}_{(n \times CO_2)} - \overline{T}_{(control)} \qquad (3.)$$

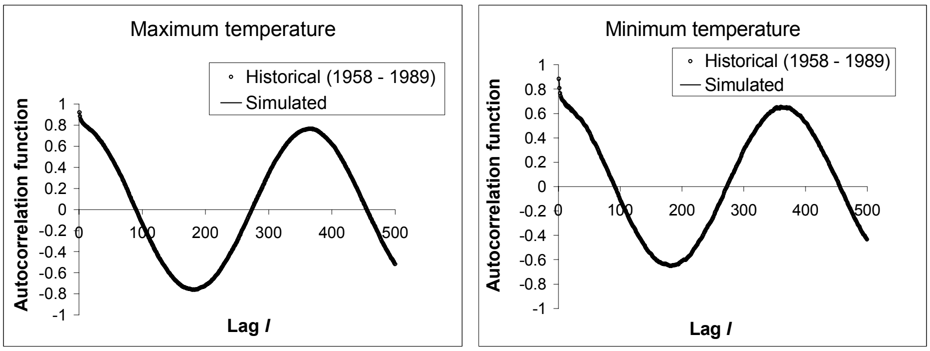


Figure 8: Comparison between observed and simulated autocorrelation function of maximum and minimum daily temperature at Borgo S. Lorenzo

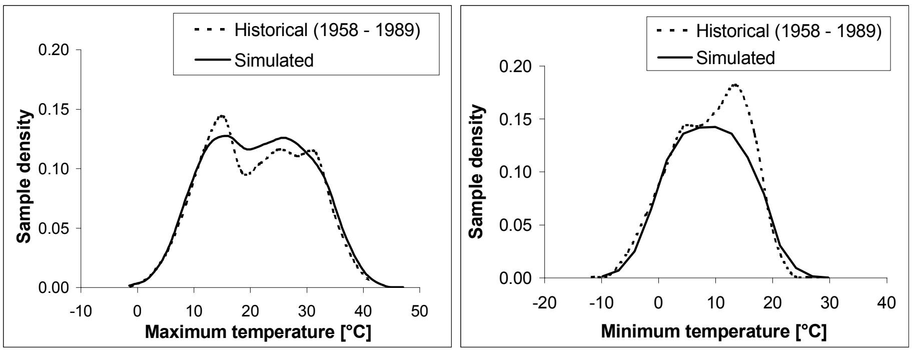


Figure 9: Comparison between observed and simulated sample probability density function of maximum and minimum daily temperature at Borgo S. Lorenzo

Table 5 displays the resulting $\Delta T$ values for all the decades representing the time horizon of the transient scenario. A series under the perturbed climate scenario has been accordingly generated covering a length of 110 years, consistently again with the rainfall transient scenario, as summarized in Table 6.

| BORGO S. LORENZO station | | |
|---|---|---|
| *Decade* | $\Delta T_{max}$ | $\Delta T_{min}$ |
| 1990-1999 | 0.50 | 0.80 |
| 2000-2009 | 0.49 | 0.83 |
| 2010-2019 | 0.96 | 1.41 |
| 2020-2029 | 1.05 | 1.50 |
| 2030-2039 | 0.90 | 1.72 |
| 2040-2049 | 1.12 | 1.64 |
| 2050-2059 | 1.87 | 2.35 |
| 2060-2069 | 2.73 | 3.42 |
| 2070-2079 | 3.19 | 3.69 |
| 2080-2089 | 3.87 | 4.31 |
| 2090-2099 | 3.71 | 4.42 |

Table 5: Decadic variations of the minimum and maximum mean temperature predicted by GCMs between control and transient scenario

| | SCENARIO | |
|---|---|---|
| VARIABLE | *Control* | *Transient* |
| Rainfall | 50 years hourly and daily rainfall | 110 years hourly and daily rainfall grouped in decades (1990-1999, 2000-2009,…) |
| Temperature | 50 years of daily maximum and minimum temperature | 110 years of daily maximum and minimum temperature grouped in decades (1990-1999, 2000-2009,…) |

Table 6: rainfall and temperature simulations performed for the Sieve river basin by means of a stochasting downscaling technique

## 2.3 Rainfall-runoff modelling

The rainfall and temperature scenarios described in the above sections have been then used to input the rainfall-runoff models to assess the impact of the enhanced $CO_2$ climate on the flood regime. The catchment response to simulated variables has been investigated according to the procedure in Figure 10.

First, a continuous simulation has been run under the control and transient scenarios by means of the PRMS - Precipitation Runoff Modeling System (*Leavesley et al.*, 1983, 1995) - which is a modular-design, distributed-parameter, physical-process model designed to evaluate the effects of various combination of precipitation, climate and land use on the runoff process. Daily discharge, evapotranspiration, soil moisture content, snowmelt, subsurface, groundwater flow and their interaction have been therefore computed for both the scenarios, so describing on a daily basis the state of the catchment.

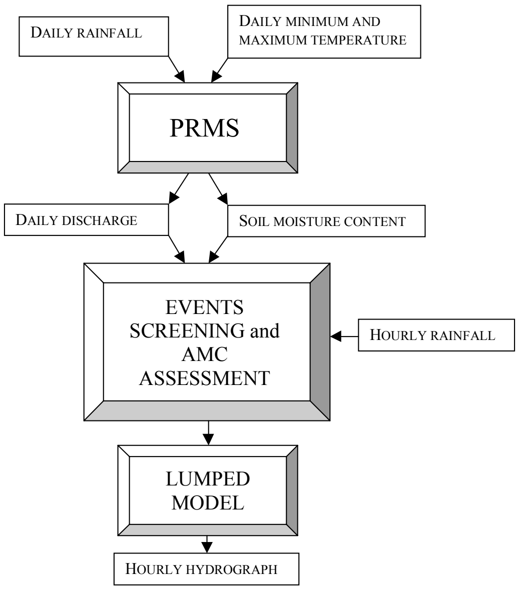


Figure 10: procedure for indirect derivation of flood peak values under control and transient scenarios

The continuous daily simulations have been subsequently used for the purpose of screening of the major rainfall events causing daily peak flows. Specifically, rainfall events to drive the lumped model have been identified by compounding within each year the information derived from the PRMS simulation and from the direct checking of precipitation patterns. Generally three events per year have been picked out, but some more have been considered any time the number of meaningful events in terms of duration and intensity has suggested that.

The hydrographs associated to each selected storm have been then reproduced by means of a lumped event-based rainfall-runoff model, coupling the SCS-CN method (*USDA*, 1972) and the Nash model (*Nash*, 1957) for net precipitation evaluation and IUH determination respectively. The estimate of the Antecedent Moisture Conditions (AMC) class, and therefore of the correct CN value to use in simulations, has been based in each case on soil moisture content simulated by PRMS and on qualitative consideration of the amount of rainfall occurred during the days preceding the event.

The maximum flow peaks among all the simulated hydrographs have been finally collected for each year, so obtaining the Annual Flood Series (AFS) under both the control and the transient scenario. Additionally to annual peak values, volume and duration have been also computed, in order to perform a comprehensive analysis of impacts of potential climate change.

| AMC class | Curve Number value | Nash **n** parameter [-] | Nash **k** parameter [h] |
|---|---|---|---|
| 1 | not considered | | |
| 2 | 72 | 3 | 2.7 |
| 3 | 79 | 3 | 2.7 |

Table 7: Estimated parameters of the lumped model.

The calibration and the validation of both the PRMS model and the event-based lumped model were previously performed on independent observed flow records. Figure 11 and Figure 12 show the fitting between simulated and measured discharge for the two models in the calibration and validation phase, while Table 7 lists the values of the parameters estimated for the Nash model and the SCS-CN method, the latter being expressed as a function of the AMC category.

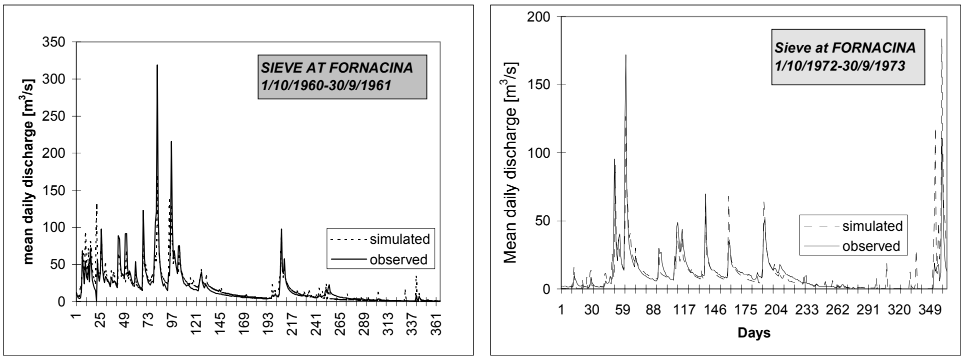


a) b)

Figure 11: examples of fitting of simulated and observed mean daily discharge for the calibration (a) and the validation (b) of PRMS model

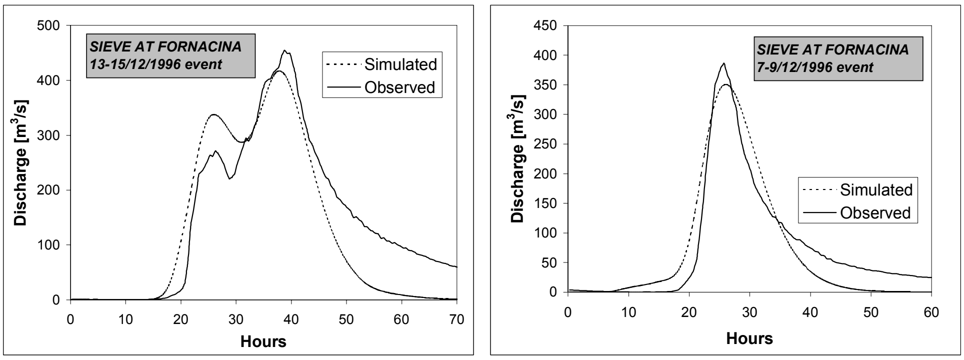


a) b)

Figure 12: examples of fitting of simulated and observed flood events for the calibration (a) and the validation (b) of the rainfall-runoff lumped model

# 3 FLOOD FREQUENCY ASSESSMENT

## 3.1 Methodology validation

A crucial point in the so far developed methodology is the capability of reproducing correctly the processes that are embedded in the growth curve of the AFS, which is an independent set of data, not used in the calibration of the procedure. It may indeed happen that the cascade modelling procedure does not capture the integral process described by the AFS, although individual processes (i.e. rainfall patterns, daily streamflow and individual flood hydrograph) are satisfactorily reproduced. Accordingly, the consistency of the flood frequency curve obtained from generated data under control scenario has been verified against the one derived from maximum annual flood peaks observed at Fornacina before assessing the potential impact of global climate change on the river basin flood regime. In this respect, the AFS dataset has been restricted to values observed between 1962 and 1986, in order to be consistent with the same temporal window on which rainfall parameters of NSRP model were calibrated. This allowed an independent verification of the reliability of the adopted modelling procedure, also highlighting major limits and the need for eventual improving corrections.

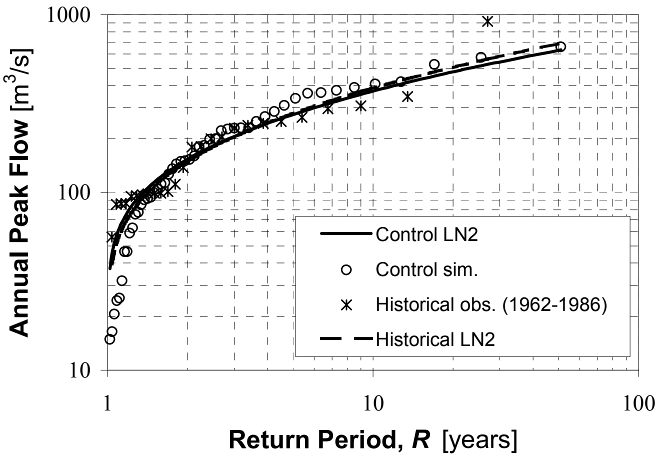


Figure 13: comparison between the flood frequency curve estimated from Fornacina cross-section AFS (1962-1986) and the flood frequency curve indirectly derived for the control scenario

As illustrated in Figure 13, the comparison between the two curves shows them to have not only similar distributional properties, both fitting a two parameters lognormal function, but also to agree quite good in shape and values along the whole range of computed return periods. This despite the curves in

Figure 13 although they originate from totally independent data sets. One could therefore conclude that the rainfall generator coupled to the rainfall-runoff methodology used to evaluate the AFS for the control scenario represents a reliable solution to reproduce at site flood frequency curves by indirect estimation methods, so enabling to use such procedure for sensitivity analysis, there including climate change impacts.

## 3.2 Impact on flood frequency

The comparison between the growth curves derived for the control and the transient scenario is shown in Figure 14 and Figure 15, this last one zooming the range of small return periods (*R* range between 1 to 10 years). Both pictures point out how flood frequency is expected to increase in the future climate, showing a trend to growth over the whole range of computed return periods, including high-frequency floods, which are usually the ones of major interest for planning purposes in areas characterized by large potential damage. Specifically, though the arising of flood values does not show meaningful variations with frequency and it averages around 50%, a slight increase of the percentage can be noticed moving from the smaller return periods (i.e. ~45% of peak flows increase for *R*=10 years) to the higher ones (i.e. ~55% for *R*=100 years). This means for instance that the 100- and 10-years quantiles respectively for the present climatic conditions are ranked as ~25- and ~4-years quantiles if a gradually changing climatic forcing would occur. On the other hand, distributional properties seem to remain unchanged, providing a two parameters lognormal probability function the best fitting also for the simulated AFS under the transient scenario.

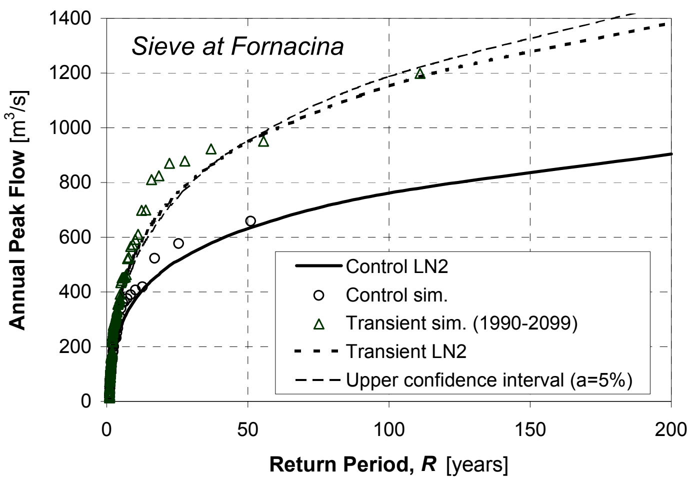


Figure 14: comparison between the flood frequency curves produced for the transient and the control climate scenario and return periods up to 200 years

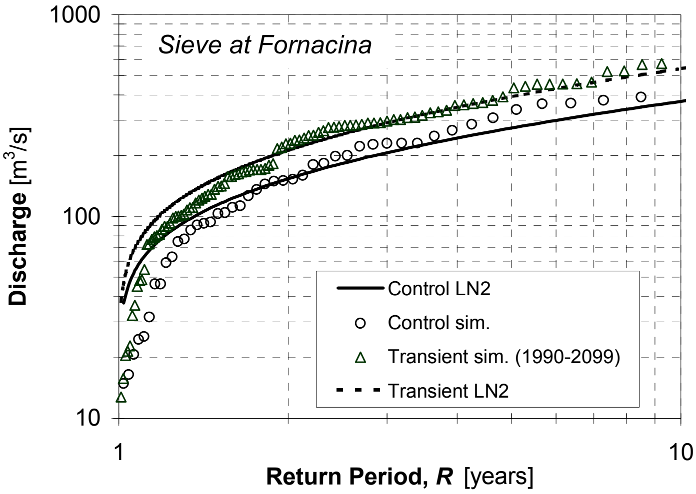


Figure 15: comparison in a log-log chart between the flood frequency curves produced for the transient and the control climate scenario and for an interval of 1 to 10 years of return period

## 3.3 Impact on flood volume and duration

Modifications to peak flows are not the only significant changes that might impact flood management policies. Flood volume and duration, i.e. the flood internal structure, might undergo changes that could as well significantly impact the overall flood risk. Accounting for process variability when generating the climate change scenario has allowed to draw some conclusions also on these two additional flood risk indicators.

In detail, the values of the two considered hydrograph properties have been computed for each event corresponding to an annual maximum flood peak and then plotted against the non-exceedance cumulative frequencies of the ranked series. Figure 16 displays the resulting curves for the flood volume under the present and future climate conditions, whereas Figure 17 reports the same plot for flood duration. The joint observation of the two figures highlights a general tendency towards flood events marked by larger volumes and longer durations, being the largest variation associated to mid-range frequencies. Such tendencies, along with a remarkably increased flood frequency, depict flood events to come in next century as characterized by an enhanced potential damaging strength, which could lead to a larger amount of damages than normally expected. This result should suggest to undertake actions aimed at increasing risk awareness and preparedness, especially if the prediction of a worsening in flood patterns will be confirmed by actual observations in coming years. A review of the current flood design philosophy, based on stationarity assumptions, should be probably accomplished, at least when designing large projects, the expected life of which goes well beyond the time horizon expected for assessing the first effects of climate change.

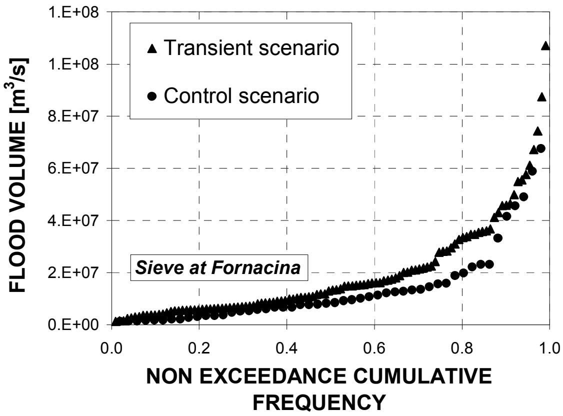


Figure 16: non-exceedance cumulative relative frequency curves of flood volume under transient and control scenarios

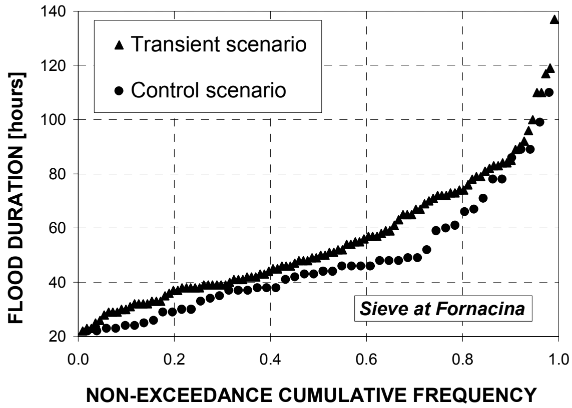


Figure 17: non-exceedance cumulative relative frequency curves of flood duration under transient and control scenarios

The dependence between flood peaks and corresponding volumes and durations has been additionally investigated, aiming at identification of potential changes in the internal evolution of a flood event. Flood volumes (Figure 18) and durations (Figure 19) are plotted to this purpose against the related annual maximum peaks. The two pictures, as one could expect, denote an evident growth of flood peak values along with both the hydrograph volume and duration. For sake of simplicity, the increasing rate is expressed by the slope of a linear regression trendline, the value of which is smaller for the transient scenario, but yet not significantly different from the one estimated for the control scenario. Specifically, data interpolations provide proportionality constants of 0.077 (control) and 0.072 (transient) $10^6 m^3/(m^3/s)$ for the peak-volume relationship and of 0.177 (control) and 0.128 (transient) hours/($m^3$/s) for the peak-duration relationship. It is however interesting to observe that altered climatic conditions seem to display a greater dispersion of the data along the trendlines with respect to a steady climate, especially apparent in the case of flood duration (Figure 19b). A possible explanation of such behaviour may be found in an increasing variance of processes underlying both changes in the rainfall internal structure and in the catchment response. The different number of simulated events (110 versus 50) considered for the modified and the unmodified scenario could also contribute, at least partially, in explaining this result.

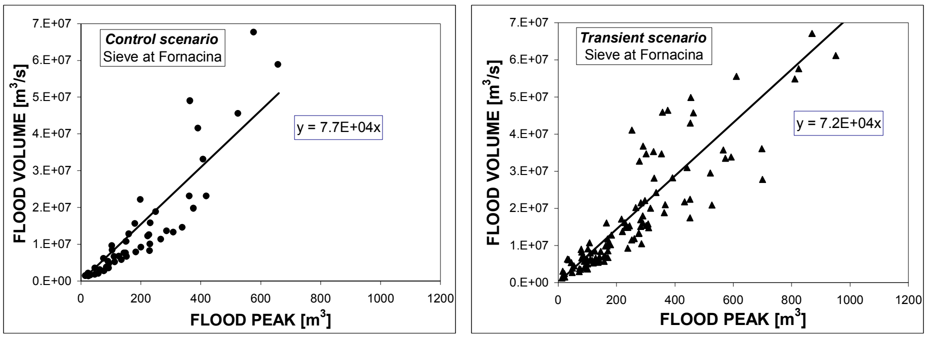


a) b)

Figure 18: flood peaks versus flood volumes of simulated events under control (a) and transient (b) scenarios

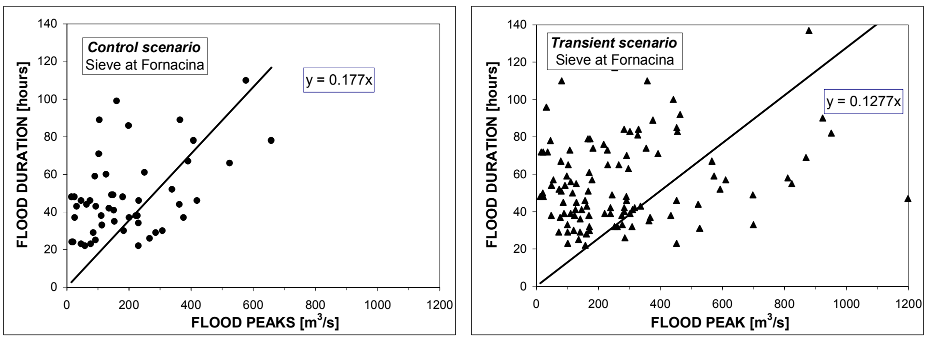


a) b)

Figure 19: flood peaks versus flood durations of simulated events under control (a) and transient (b) scenarios

## 3.4 Impact on Peaks Over Threshold (POT)

The traditional AFS analysis has been finally integrated by an investigation about changes on the number of events above given threshold of peak discharge. The prediction of a future hit by annual maximum floods with potential higher risk, larger volumes and longer durations, suggests indeed that other menacing extreme events could take place within each single year. In order to evaluate the occurrence rate of critical events, the number of Peaks Over Threshold (POT) has been then evaluated for the two climatic scenarios under study on the basis of the mean daily discharge series provided by the PRMS model. Several thresholds between 50 and 100 $m^3/s$ have been considered as illustrated by Table 8, where the POT totals obtained for each threshold are reported. Table 9 lists the mean annual POT values averaged on 110 and 50 years simulation periods for the transient and the control scenario respectively. Figure 20 shows the absolute and percentage difference existing in the mean annual POT for the same two $CO_2$ scenarios. As expected, mean annual POT are subject to a general increase in value under global climate change, which is variable depending on the threshold. The differences between mean values range from 1.14 events per year for the 50 $m^3/s$ threshold to 0.43 events per year for the 100 $m^3/s$ one. Therefore, the catchment response seems to show a greater sensitivity to global change when higher-frequencies flood events are most likely to occur, as clearly showed in Figure 20. This might certainly have many potential implications in civil and environmental engineering design problems, such as mechanical stress and maintenance of flood protection structures, erosion and sediment transport, and, more in general, flood mitigation strategies.

| | *Peaks Over Threshold totals* | | | | | |
|---|---|---|---|---|---|---|
| *Threshold* [$m^3/s$] | *50* | *60* | *70* | *80* | *90* | *100* |
| Control scenario | 211 | 155 | 109 | 74 | 51 | 35 |
| Transient scenario | 590 | 434 | 316 | 243 | 166 | 124 |

Table 8: total number of Peaks Over Threshold values observed in the daily discharge series simulated by the PRMS model for different thresholds and scenarios

| | *Mean Annual Peaks Over Threshold* | | | | | |
|---|---|---|---|---|---|---|
| *Threshold* [$m^3/s$] | *50* | *60* | *70* | *80* | *90* | *100* |
| Control scenario | 4.22 | 3.1 | 2.18 | 1.48 | 1.02 | 0.7 |
| Transient scenario | 5.36 | 3.95 | 2.87 | 2.21 | 1.51 | 1.13 |

Table 9: mean annual Peaks Over Threshold values observed in the daily discharge series simulated by the PRMS model for different thresholds and scenarios

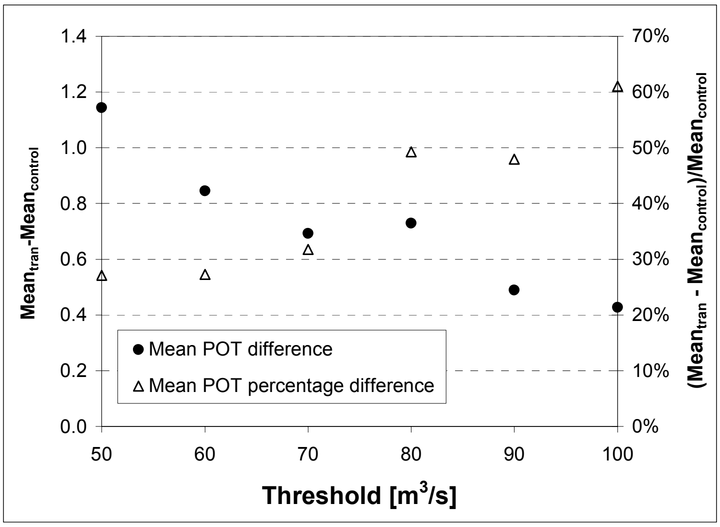


Figure 20: absolute and percentage differences of mean annual POT values for different thresholds under the transient and the control scenario

Finally, Figure 21 reports the patterns of mean annual POT values over the decades of the transient scenario for several thresholds (50, 90 and 100 $m^3/s$). Suprisingly, this does not show a time-dependent trend, and exhibits rather a strong fluctuating behaviour which reaches its maximum during the 2030-2039 decade. It also displays a smoothing tendency for higher thresholds, definitely suggesting that process variability can not be neglected from any speculation on climate change impact assessment.

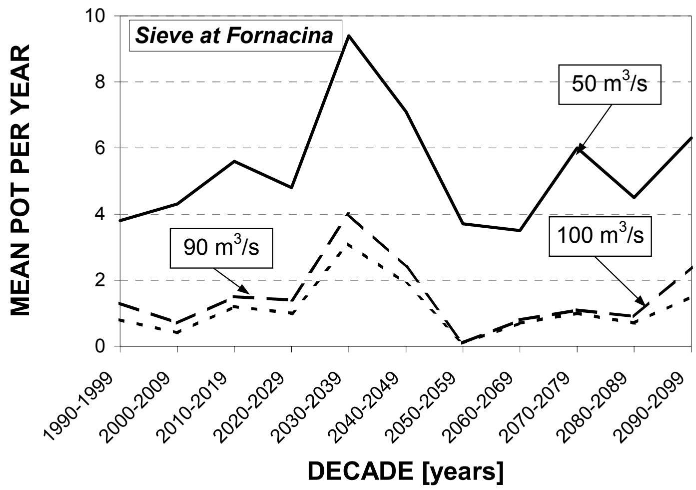


Figure 21: variation of decadic mean annual POT values for the transient scenario

# 4 CONCLUDING REMARKS

In the present study local potential climatic changes due to the increase of the greenhouse effect and their impact on flood regime have been extensively analyzed for the Sieve river basin (Central Italy). GCMs predictions coupled to stochastic downscaling techniques are used to reproduce realistic projections of rainfall and temperature patterns at the basin scale. Two climatic scenarios have been considered: the control scenario, which is expected to represent current climate with a constant atmospheric $CO_2$ concentration, and the transient scenario, in which the climatic forcing due to the joint effect of greenhouse gases and sulphate aerosols is gradually increased, so reflecting, a more realistic climate evolution than the usual assumption of a steady state doubled $CO_2$ climate. Point long-term simulations of maximum and minimum daily temperature and of rainfall at a hourly resolution have been then performed under both scenarios for a climatic station which is approximately located in the center of the basin. In a second time, these are given as inputs to serially combined rainfall-runoff models in order to investigate induced variations on the catchment response and, above all, on floods generation and occurrence. Main hydrograph characteristics of maximum annual flood events, that is flood peak, volume and duration, are computed for stationary and non-stationary climatic conditions, so providing the necessary elements to carry out a comprehensive analysis on how frequencies of occurrences, distributional properties and internal structure of the flood events might change.

The confidence in the reliability of the adopted procedure has been first investigated to avoid the introduction of uncontrolled and/or undesired model biases. The flood frequency curve simulated for the control scenario has been thus first validated against the one derived from the observed AFS, obtaining a good agreement, especially considering that it has been derived from a dataset independent form AFS. Therefore the adopted methodology, despite its simplicity, has been assumed to be a robust technique to fairly reproduce at site AFS growth curves.

As for the impact of climate change on flood regime of the Sieve river basin, the potential future extreme events are generally characterized by higher peaks, larger volumes and longer durations. For instance, both low and high frequency peak values indicate an increase of about 50% for a given return period, while flood volumes and durations arise especially with respect to mid-range frequencies. A worsening effect under climate change is however remarkable over the whole range of considered return periods (1 to 100 years), that is the range of interest for technical purposes. The analysis of the hydrograph internal structure seems to conduct toward bigger uncertainty in defining peak-volume and peak-duration relationships, due to the more scattered patterns that flood volumes and durations show in the transient scenario than in the control one, so outlining an enhanced variability of the process. Finally, the evaluation of the mean annual Peaks Over Threshold denotes again a significantly increase induced by the effects of enhanced $CO_2$ atmospheric concentration on climate, especially concerned with smaller thresholds, so suggesting a larger frequency of events potentially leading to flood dangers.

The above considerations underline the considerable impact that climate change could have on the generation of extreme flood events, with special respect to their occurring frequencies, intrinsic structural properties and related risk. Although major criticisms to climate change impact assessment confine many results from this research field to speculation, the outcomes of this study point out that the system might react to climate change showing effects that can be, in some cases, unexpected. Even in the case of skeptical attitude with respect to potential climate change, these results can show how strong could be the effects of non stationarities due to natural fluctuations of climate, the order of magnitude of which can be similar to expected anthropogenic climate change. Therefore, policy makers and designers are here offered to become aware about what non-stationarity of climate – whichever the cause – could lead to. Current flood design criteria as well as general water resource management strategies should be on this basis questioned, addressing their adequacy to face a system evolution which does not comply with the traditional view of process stationarity.

A convincing argument in this respect could stem from the fact that the adopted procedure takes into account the local seasonality and the non-stationarity of hydrological variables by making use of predictions based on a gradually changing climatic forcing. These two features, reflecting the actual behaviour of natural processes, are recognized to be key elements for reproducing on a regional scale future climate scenarios as realistic as possible (*Mitchell et al.*, 1995).

On the other hand it must be however recognized that a number of limitations still characterizes climate change impact assessment even in the case of advanced analysis like the present one. For instance one could to notice that feedback effects are not considered, neither at the global nor at the local scale. The basin under study is forced to keep constant his responding behaviour, assuming that no relevant influence on extreme floods generation could be caused by feedback mechanisms on the soil characteristics and their interactions with the atmosphere.

Concluding, the present work, far from giving the final answer to the solution of the complex problem of assessing climate change impact on local flood regime, presents a simple, but robust analysis tool to investigate the catchment response to climatic fluctuations, which could represent a valid alternative until better understanding of the complex phenomenology of flood formation will allow the application of more sophisticated methodologies. Unfortunately, though very significant improvements were made in the past decades, big uncertainties still dominate the reproduction of climatic change scenarios by GCMs and the modelling of hydrological processes. Further research is therefore needed to understand and, when possible, to quantify how much such uncertainties weight on the evaluation of flood regime variations induced by climate change.

Acknowledgments: The present study has been developed under the support of seed funding money the Alliance for Global Sustainability funding money at ETH Zürich (funding 2-85227-98). Dr. David Viner of the University of East Anglia and the UK Meteorological Office are kindly acknowledged for allowing the use of HADCM2 simualtions.

## REFERENCES

Askew, A.J. Climate Change and water resources, The influence of climate change and climatic variability on the hydrologic regime and water resources, Proceedings of the Vancouver Symposium, IAHS Publ. No. 168, pp. 421-430, 1987.

Beniston, M. From turbulence to climate, Springler Verlag, berlin-Heidelberg-New York, 1998.7

Brandsma, T. & Buishand, T.A. KNMI contribution to the European project POPSICLE, Tech. Rep. TR-194, KNMI, De Bilt, The Netherlands, 1996.

Brandsma, T. & Buishand, T.A. Dependence of precipitation on temperature at Florence and Livorno (Italy), *Climate Research*, 1999, **12**(6), 53-63.

Burlando, P. Modelli matematici per la previsione e la simulazione della precipitazione nel tempo, Ph.D. dissertation (in Italian), Institute of Hydraulics, Politecnico di Milano, Milano, Italy, 1989.

Burlando, P. & Rosso, R. Investigating temporal rainfal patterns under different climate change scenarios via re-scaling point process models, paper presented at the Chapman Conf. on "Hydrologic Aspects of Global Climate Change", Am. Geoph. Union, Lake Chelan, June 12-14, unpublished manuscript, November, 1990.

Burlando, P. & Rosso, R. Extreme storm rainfall and climate change, *Atmospheric Research*, 1991, 27, 169-189.

Burlando, P. & Rosso, R. Stochastic Models of Temporal Rainfall: Reproducibility, Estimation and Prediction of Extreme Events, *Stochastic Hydrology and its Use in Water Resources Systems Simulation and Optimization,* ed. by J.D. Salas, R. Harboe and J. Marco-Segura, Proc. of the NATO-ASI Workshop, Peñiscola, Spain, September 18-29, 1989, Kluwer Ac. Publ., Dordrecht, The Netherlands, 1993, pp.137-173.

Burlando, P., Grossi, G., Montanari, A. & Rosso R. POPSICLE – Production Of Precipitation Scenarios for Impact assessment of CLimate Change in Europe, CIRITA final report, Milano, April 1997.

Burton, I. Vulnerability and adaptive response in the context of climate and climate change, *Climatic Change*, 1997, 36, 185-196.

Cohen, S.J. Impacts of CO2-induced climatic change on water resources in the Great Lakes Basin, *Climatic Change*, 1986, 8, 135-153.
Cowpertwait, P.S.P. A generalized point process model for rainfall, *Proc. of R. Soc. Lond.*, 1994, 447, 23-37.
Cowpertwait, P.S.P. A generalized spatial-temporal model of rainfall based on a clustered point process, *Proc. of R. Soc. Lond.*, 1995, 163-175.
Cowpertwait, P.S.P., O'Connell, P.E., Metcalfe, A.V. & Mawdsley, J. Stochastic point process modelling of rainfall, *J. Hydrol*. 1996, 175, 17-65.
De Michele, C., Montanari, A. & Rosso, R. The effects of non-stationarity on the evaluation of critical design storms, *Wat. Sci. Tech*., 1998, **37**(11), 187-193.
Epstein D. & Ramirez J.A. Spatial disaggregation for studies of climatic hydrologic sensitivity, *J. Hydr. Eng.*, 1994, **120**(12), 1449-1467.
Giorgi, F. & Mearns, L.O. Approaches to the simulation of regional climate change: a review, *Rev. Geoph.*, 1991, 29, 191-216.
Gleick, P.H. Global climatic changes and regional hydrology: impacts and responses, The influence of climate change and climatic variability on the hydrologic regimes and water resources, Proceeding of the IAHS Vancouver Symposium, August 1987, IAHS Publ. No. 168, 389-402.
Gleick, P.H. Climate change, hydrology and water resources, *Rev. Geophys.*, 1989, **27**(3), 329-344.
Gupta, V.K. & Waymire, E. Multiscaling properties of spatial rainfall and river flow distributions, *J. Geophys. Res.*, 1990, **95**(D3), 1999-2009.
Hughes, J.P., Lettenmaier, D.P. & Guttorp, P. A stochastic approach for assessing the effect of changes in synoptic circulation patterns on gauge precipitation, *Water Resour. Res*., 1993, **29**(10), 3303-3315.
IPCC. IPCC Technical guidelines for assessing climate change impacts and adaptations, Ed. by T.R. Carter, M.L. Parry, H. Harasawa, S. Nishioka, University College Londono and Centre for Global Environmental Research, 1994.
IPCC. Climate Change 1995: The Science of Climate Change, contribution of Working Group I to the *Second Assessment Report of The Intergovernmental Panel on Climate Change*, Ed. by J.J. Houghton, L.G. Meiro Filho, B.A. Callander, N. Harris, A. Kattenberg and K. Maskell, 1995a.
IPCC. Climate Change 1995: Impacts, Adaptations and Mitigation of Climate Change. Scientific-Technical Analyses, Contribution of Working Group II to the *Second Assessment Report of The Intergovernmental Panel on Climate Change*, Editors R.T. Watson, M.C. Zinyowera and R.H. Moss, 1995b.
IPCC Climate Change 1995: Economic and Social Dimension of Climate Change, Contribution of Working Group III to the *Second Assessment Report of The Intergovernmental Panel on Climate Change*, Ed. by J. Bruce, Hoesung Lee and E. Haites, 1995c.

Klemes V. Sensitivity of water resource systems to climate variations, World Climate Applications Programme, WCP 98, World Meteorological Organization, Geneva, Switzerland.
Kottegoda, N.T. Stochastic water resources technology, The MacMillan Press LTD, London, 1980.
Leavesley, G.H., Lichty, R.W., Troutman, B.M. & Saindon, L.G. Precipitation-Runoff Modelling System: User's Manual, U.S. Geological Survey Water Resourced Investigations Report, 1983.
Leavesley, G.H. & Stannard, L.G. The Precipitation-Runoff Modelling System - PRMS, *Computer Models of Watershed Hydrology*, ed. by V.P. Singh, Water Resour. Publ., Highland Ranch, Colorado, USA, 1995, pp. 281-310.
Lettenmaier, D.P. & Gan, T.Y. Hydrologic sensitivity of the Sacramento-San Joaquin river basin, California, to global warming, *Water Resour. Res.*, 1990, **26**(1), 69-86.
Loukas, A. & Quick, M.C. Effect of climate change on hydrologic regime of two climatically different watersheds, *J. of Hydrol. Eng.*, 1996, **1**(2), 77-87.
Loukas, A. & Quick M.C. The effect of climate change on floods in British Columbia, *Nordic Hydrology*, 1999, 30, 231-256.
Mearns, L.O., Rosenzweig, C. & Goldberg, R. Mean and variance change in climate scenarios: methods, agricultural applications, and measures of uncertainty, *Climatic Change*, 1997, 35, 367-396.
Mimikou, M. & Kouvopoulos, Y.S. Regional climate change impacts: 1. Impacts on water resources, *Hydrol. Sci. J.*, 1991, 36, 247-258.
Mitchell, J.F.B. The "greenhouse" effect and climate change, Reviews of Geophysics, 1989, 27, 115-139.
Mitchell, J.F.B., Johns, T.C., Gregory, J.M. & Tett, S.F.B. Climate response to increasing levels of greenhouse gases and sulphate aerosols, *Nature*, 1995, 376, 501-504.
Nash, J.E., The form of the istantaneous unit hydrograph, IASH publication n. 45, 1957, vol. 3-4, 114-121.
Nash, L.L. & Gleick P., Sensitivity of streamflow in the Colorado basin to climatic changes, *J. Hydr.*, 1991, 125, 221-241.
Nemec, J. & Schaake, J.C. Sensitivity of water resource system to climate variations, *Hydrol. Sci. J.*, 1982, 27, 327-343.
POPSICLE. Production of precipitation scenarios for impact assessment of climate change in Europe, Final report to the European Union of the project POPSICLE, Contract EV5V-CT94-0510, European Commission, DGXII, Environment and Climate, Brussels, 1997.
Quick, M.C. the U.B.C. Watersheds Model, In V.P. Singh (Ed.) Computer models of watersheds hydrology, Water Resource Publications, Colorado, USA, 1995.
Ripley, E.A. Climatic change and the hydrologic regime, M.C. Healey and R.R. Wallace (Eds.), *Canadian Aquatic Resources*, Department of Fisheries and Oceans, Ottawa, ON, 1987, 137-178.

Rodriguez-Iturbe, I., Scale of fluctuation of rainfall models, *Water Resour. Res.*, 1986, **22**(9), 15S-37S.

Semenov M.A. & Barrow E.M. Use of a stochastic weather generator in the development of climate change scenarios, *Climatic Change*, 1997, 35, 397-414.

Strzepek, K.M. & Yates, D. Climate Change impacts on the hydrologic resources of Europe: a simplified continental scale analysis, *Climatic Change*, 1997, 36, 79-92.

USDA (U.S. Department of Agricolture), Soil Conservation Service. National Engineering Handbook, Hydrology, Sect. 4, Washington D.C., 1972.

Vanmarcke, E. Random Fields: analysis and synthesis, MIT Press, Cambridge, Massachusetts, 1983.